Coulomb effects in the absorbance spectra of two-dimensional Dirac materials

Coulomb effects in the absorbance spectra of two-dimensional Dirac materials

Leone Di Mauro Villari, Ian Galbraith, and Fabio Biancalana
Institute of Photonics and Quantum Sciences, School of Engineering and Physical Sciences, SUPA, Heriot-Watt University, Edinburgh EH14 4AS, United Kingdom

(Received 17 May 2018; revised manuscript received 8 October 2018; published 2 November 2018)

A wide range of materials like graphene, topological insulators, and transition-metal dichalcogenides (TMDs) share an interesting property: the low-energy excitations behave as Dirac particles. This emergent behavior of Dirac quasiparticles defines a large class of media that are usually called Dirac materials. In this work we build the foundations of a way to study the linear optical properties of these two-dimensional media. Our approach is based on a Dirac-like formulation of the standard semiconductor Bloch equations used in semiconductor physics. We provide an explicit expression of the linear absorbance, which we call the relativistic Elliott formula, and use it to quantify the variation of the continuum absorbance spectrum with the strength of the Coulomb interaction (the Sommerfeld factor). Our calculations also show how the Coulomb enhancements scales with the band gap and vanishes for zero band gap, shedding light on the behavior of graphene for low-light intensities. The results presented are in good quantitative agreement with published experimental results. Our theory can help researchers to explore the nonlinear interactions of intense, ultrashort pulses with TMDs, and the framework is flexible enough to be adapted to different experimental situations, such as cavities, multilayers, heterostructures, and microresonators.

DOI: 10.1103/PhysRevB.98.205402

I. INTRODUCTION

Condensed-matter physics is witnessing rapid expansion in the fabrication of a wide variety of materials with Dirac fermion quasiparticle excitations. These seemingly diverse materials possess properties that are a direct consequence of the Dirac spectrum of the quasiparticles and are universal. For example, neutral superfluid d-wave superconductors and graphene, which are characterized by a massless Dirac fermion low-energy spectrum, all exhibit the same power-law temperature dependence of the fermionic specific heat, with the only differences arising from the dimensionality of the excitation phase space [1]. Among Dirac materials, gapless graphene is one of the most widely studied due to its unusual physical properties arising from the interplay of its reduced dimensionality and the nature of its excitation spectrum [2–5].

Perhaps the most intriguing characteristic of graphene is the so-called universal absorbance. The opacity of suspended graphene is defined solely by the fine-structure constant ($\alpha = e^2/\hbar c$), the parameter that describes coupling between light and relativistic electrons which is traditionally associated with quantum electrodynamics (QED) rather than materials science [4]. This universal behavior is known to be broken by opening a gap, with the appearance of bound states (excitons) due to the electron-hole Coulomb interactions. A gap can be opened in graphene when the sample is deposited on a dielectric substrate [6], or it can be induced by impurities, lattice defects [7], and mechanical strain [8]. In terms of the low-excitation Dirac Hamiltonian the effect of a gap opening is analogous to the chiral symmetry breaking in QED that generates a mass gap in the particle-antiparticle spectrum [9,10]. This suggests that fermions in gapped graphene can be accurately described by a massive Dirac Hamiltonian. Even if gapped graphene remains the best example for the massive Dirac model, another class of two-dimensional materials whose low-energy excitations can be described as massive Dirac particles is provided by monolayer transition-metal dichalcogenides (TMDs) such as molybdenum disulfide (MoS_2) and tungsten diselenide (WSe_2) [11–15]. Akin to graphene, these materials display new physical properties, distinct from their bulk counterparts [11,16–19]. Here, emission is dominated by excitons and trions due to the strong Coulomb interactions arising from their low dimensionality and reduced dielectric screening. Remarkably, despite their tiny atomic thickness they can absorb up to 20% of the incident light [18,19]. Proper analysis of the measured spectra requires the identification of the optically active states. For this purpose, one derives dipole-allowed selection rules that result from the conservation of the total angular momentum in the excitation and emission processes. In conventional direct-gap GaAs-type quantum wells the radial nature of the dipole moment imposes that only s-type excitonic states couple to light [13,20]. This leads to the well-known excitonic Rydberg series. It has been shown that in the case of monolayer TMDs in the regime of strong Coulomb interactions the system collapses into a excitonic insulator phase and optically bright p excitons are allowed [13]. However recent works pointed out that for a gapped Dirac system the symmetry properties of the $\boldsymbol{K}$ point result in a nonradial dipole moment with a nontrivial angular dependence related to the appearance of a Berry phase [21]. This peculiar characteristic suggests that different dipole-allowed transitions should be present and optically active p states should appear even in the weak Coulomb interaction regime. These states are predicted by our theory, but their

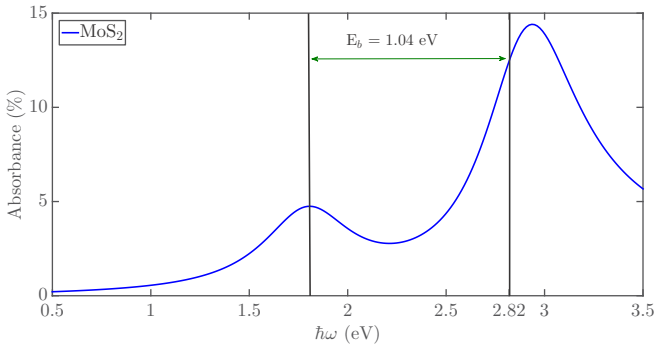

FIG. 1. Plot of the absorbance [Eq. (13)] using parameters for a MoS_2 TMD on a fused-silica substrate: energy gap $\Delta = 2.82\,\mathrm{eV}$ and background refractive index $n_b = 1.5$. We use a $\delta = 0.1\Delta$ Lorentzian broadening on both exciton and continuum transitions. E_b is the binding energy for the $1s$ Dirac exciton.

oscillation strength is very low when compared with the $1s$ exciton state, and we will disregard them in the rest of the paper.

So far optical properties of TMDs have been extensively studied by using the semiconductor Bloch equations (SBEs) [22–24], the equivalent Bethe-Salpether equation, and the GW approximation [23,25], detailing the exciton physics, the optical absorption [22,23,25], and the second-harmonic generation [24].

In this paper we propose a formalism to study the optical properties of Dirac materials in the theoretical framework of the instantaneous eigenstates [26], and we apply this formalism to predict the spectra of realistic materials. We derive the Elliott formula for a gapped Dirac system taking into account both the discrete and continuum parts of the Wannier eigenvalue problem. In particular we study how the absorbance spectrum evolves as the band gap is reduced to zero. We show that even in the presence of relatively strong electron-hole Coulomb interaction the gap reduction leads to the universal absorbance of graphene, and we show how this behavior is closely related to the structure of the relativistic hydrogenic problem.

Before detailing our calculations we show in Fig. 1 the absorbance spectrum calculated for the molybdenum disulfide (MoS_2). We observe a high absorbance value (15%) around the energy gap, in agreement with previous experimental and theoretical results [19,27,28]. The intensity of the continuum absorbance peak is around three times stronger than the $1s$ exciton one. This is a peculiar characteristic shared by materials with a Dirac-like low-energy spectrum. In what follows we show how the continuum absorbance relates to the relativistic structure of the low-energy quasiparticle excitations. It is possible to attribute the high absorbance rate at the band edge to so-called C-exciton peaks that are beyond the theory presented here [25,29,30]. C excitons arise from particle-hole excitations in a circular region of the Brillouin zone centered at the $\boldsymbol{K}$ points with a maximal contribution from the regions between $\boldsymbol{\Gamma}$-$\boldsymbol{K}$ and $\boldsymbol{M}$-$\boldsymbol{K}$ [30]. From this observation it is clear that a theory concerning only the excitations around the $\boldsymbol{K}$ point is not able to capture the physics beyond these exciton peaks. Notably, our theory still predicts a significant enhancement at the band edge entirely related to relativistic continuum states even if it cannot account for the more than 40% absorption peak observed in MoS_2. This seems to indicate that continuum states give a substantial contribution to the high band-edge absorbance, which would be an addition to absorption arising from C excitons.

II. RENORMALIZED DIRAC-BLOCH EQUATIONS

The starting point for our analysis is the low-energy Hamiltonian for the band structure in the vicinity of the Dirac points ($\mathbf{k} = 0$). Governed by the symmetry properties of the hexagonal lattice, the lowest-order $\mathbf{k}\cdot\mathbf{p}$ Hamiltonian including the light-matter interaction and neglecting the spin-orbit interaction has the form

$$H_{\mathbf{k}} = v_F\left[\boldsymbol{\sigma}\cdot\left(\hat{\mathbf{p}} + \frac{e}{c}\mathbf{A}(t)\right)\right] + \sigma_z\frac{\Delta}{2} + I_2 V(\mathbf{r}), \tag{1}$$

where v_F is the Fermi velocity, $\mathbf{A}(t)$ is the vector potential, Δ is the energy gap, I_2 is the 2×2 identity matrix, $V(\mathbf{r})$ is the electrostatic potential, $\boldsymbol{\sigma} = (\sigma_x, \sigma_y)$ are the first two Pauli matrices, and σ_z is the third one. The usual approach used to study the optical properties of this Hamiltonian parallels that of the SBEs [31]. However, recent works show that a full understanding of the nonlinear optics of Dirac materials requires one to go beyond the SBEs [21,26,32]. In 2010 Ishikawa derived an extended version of the SBEs for graphene using the formalism of instantaneous eigenstates [26] which has recently been generalized for a gapped material [21].

The theory developed in these works unveils novel and previously unexplained nonlinear optical properties of graphene and gapped graphene; however, they do not include Coulomb interactions that are, in general, very strong in two-dimensional semiconductors, preventing meaningful predictions from being made. The inclusion of Coulomb interactions within this formalism requires the second quantization of Hamiltonian (1). To accomplish this, we need to quantize the instantaneous Dirac field; the procedure is simple but rather lengthy (see Appendix A), and it results in the second quantized Hamiltonian

$$H = \sum_{\mathbf{k}} \epsilon_{\mathbf{k}}(t)(\hat{a}^\dagger_{\mathbf{k}}\hat{a}_{\mathbf{k}} - \hat{b}^\dagger_{-\mathbf{k}}\hat{b}_{-\mathbf{k}}) - \hbar\Omega_{\mathbf{k}}(t)(\hat{a}^\dagger_{\mathbf{k}}\hat{b}_{-\mathbf{k}} + \mathrm{H.c.}), \tag{2}$$

where $a_{\mathbf{k}}$ and $b_{\mathbf{k}}$ are, respectively, the annihilation operators for electrons and holes and $\epsilon_{\mathbf{k}}(t) = \pm\sqrt{v_F^2|[\mathbf{p} + e/c\mathbf{A}(t)]|^2 + \Delta^2/4}$ and $\Omega_{\mathbf{k}}(t) = ev_F E(t)/\hbar[\sin\phi_{\mathbf{k}}/(2\epsilon_{\mathbf{k}}) - i\Delta\cos\phi_{\mathbf{k}}/(4\epsilon_{\mathbf{k}}^2)]$ are the instantaneous energy and Rabi frequency, respectively, with $\phi_{\mathbf{k}} = \arctan(k_y/k_x)$. This Hamiltonian differs from the usual second quantized two-dimensional (2D) semiconductor case because both $\epsilon_{\mathbf{k}}(t)$ and $\Omega_{\mathbf{k}}(t)$ explicitly depend on the interaction field $\mathbf{A}(t)$. The presence of the Coulomb potential $V(\mathbf{r})$ leads to a renormalization of both the instantaneous energy and the Rabi frequency. Introducing the microscopic polarization $p_{\mathbf{k}} = \langle\hat{b}_{-\mathbf{k}}\hat{a}_{\mathbf{k}}\rangle$ and the electron-hole occupation numbers $n^e_{\mathbf{k}} = \langle\hat{a}^\dagger_{\mathbf{k}}\hat{a}_{\mathbf{k}}\rangle$, $n^h_{\mathbf{k}} = \langle\hat{b}^\dagger_{-\mathbf{k}}\hat{b}_{-\mathbf{k}}\rangle$ we can show that they satisfy the following system of *renormalized Dirac-Bloch*

(RDB) equations:

$$\begin{aligned}\hbar\dot{p}_{\mathbf{k}} &= -2i\,\epsilon^R_{\mathbf{k}}(t)p_{\mathbf{k}} - i\hbar\Omega^R_{\mathbf{k}}(t)e^{i2\gamma_{\mathbf{k}}}\left(n^e_{\mathbf{k}} + n^h_{\mathbf{k}} - 1\right),\\ \dot{n}^{e,h}_{\mathbf{k}} &= -2\,\mathrm{Re}\left[\Omega^R_{\mathbf{k}}(t)\right]\mathrm{Im}(p_{\mathbf{k}}e^{i2\gamma_{\mathbf{k}}})\\ &\quad -4\,\mathrm{Im}\left[\Omega^R_{\mathbf{k}}(t)\right]\mathrm{Re}(p_{\mathbf{k}}e^{i2\gamma_{\mathbf{k}}}),\end{aligned} \tag{3}$$

where $\epsilon^R_{\mathbf{k}}(t) = \epsilon_{\mathbf{k}}(t) + \sum_{\mathbf{k}'\neq\mathbf{k}} V_{|\mathbf{k}-\mathbf{k}'|}(n^e_{\mathbf{k}'} + n^h_{\mathbf{k}'} - 1)$ and $\Omega^R_{\mathbf{k}}(t) = \Omega_{\mathbf{k}}(t) + 1/\hbar\sum_{\mathbf{k}'\neq\mathbf{k}} V_{|\mathbf{k}-\mathbf{k}'|}p_{\mathbf{k}'}$ are the renormalized energy and Rabi frequency. The phase term $\gamma_{\mathbf{k}}$ is a gap-induced Berry phase (see Appendix A for details). The formulation of Eqs. (2) and (3) is the first result of this paper. As was the case for the SBEs [31,33–35], the RDB equation framework can be flexibly applied to many optical pulsed experiments and can provide a route to the microscopic understanding of linear and nonlinear properties of gapped TMDs. This approach will pave the way for a deeper understanding of the excitonic structure and the interaction of ultrashort, intense light pulses with Dirac materials.

A word of caution is in order: the gapped Dirac Hamiltonian is only a first-order $\mathbf{k}\cdot\mathbf{p}$ approximation of the full tight-binding Hamiltonian and accounts only for its centrosymmetric part. Several works (e.g., Refs. [11–15]) use this Hamiltonian to model TMD monolayers. Such an approximation for TMDs, like the simple parabolic one that is also used to model TMDs, e.g., in Ref. [32], is adequate only to describe properties of such media that are accounted for by low momentum states, where this approximation is accurate. It is, nonetheless, clearly insufficient to accurately capture the full first-principles band structure, for which higher-order terms in the $\mathbf{k}\cdot\mathbf{p}$ expansion must be considered [36].

III. LINEAR ABSORPTION

As a first example of the practical application of our equations, we now consider the RDB equations in the low-intensity and low-density limit $[e/cA(t) \ll \Delta/(2v_F)$ and $n^e_{\mathbf{k}} - n^h_{\mathbf{k}} = -1]$ where only the polarization equation survives. We will also assume a continuous-wave radiation field. This will allow us to explore analytically excitonic effects on the linear optical properties of gapped TMDs (a detailed calculation is given in Appendix B). Equation (3) then reduces to

$$i\hbar\frac{d}{dt}p_{\mathbf{k}} = -2\left(\epsilon_{\mathbf{k}} + \sum_{\mathbf{k}'\neq\mathbf{k}} V_{|\mathbf{k}-\mathbf{k}'|}\right)p_{\mathbf{k}} + \hbar\Omega^R_{\mathbf{k}}(t)e^{i2\gamma_{\mathbf{k}}}, \tag{4}$$

with the nonrenormalized energy reducing to $\epsilon_{\mathbf{k}} = \sqrt{v_F^2\mathbf{p}^2 + \Delta^2/4}$. This equation is associated with the well-known Wannier stationary eigenvalue problem, which, for a massive Dirac quasiparticle reads

$$\left[-iv_F\hbar\,\boldsymbol{\sigma}\cdot\boldsymbol{\nabla} + \sigma_z\frac{\Delta}{2} + V(\mathbf{r})\right]\vec{\Psi}_\nu(\mathbf{r}) = E_\nu\vec{\Psi}_\nu(\mathbf{r}), \tag{5}$$

where $\vec{\Psi}_\nu(\mathbf{r})$ $(\nu = n, j)$ is a two-component spinor eigenfunction of the electron-hole pair states which in polar coordinates has the form

$$\vec{\Psi}_\nu(\mathbf{r}) = \begin{pmatrix} e^{i(j+1/2)\phi_{\mathbf{r}}}\,F_\nu(r) \\ \pm ie^{i(j-1/2)\phi_{\mathbf{r}}}\,G_\nu(r)\end{pmatrix}, \tag{6}$$

where $j = m + 1/2$ is the eigenvalue of the "isospin-angular" momentum $\hat{J}_z = \hat{L}_z + \frac{1}{2}\sigma_z$ along the z axis and n is the principal quantum number. The corresponding eigenvalues are

$$E_\nu = \hbar\omega_\nu = \frac{\Delta}{\sqrt{1 + \frac{\alpha_c^2}{(n+\gamma)^2}}}, \tag{7}$$

with $\gamma = \sqrt{j^2 - \alpha_c^2}$. The constant α_c is the dimensionless Coulomb coupling strength and is determined by the background dielectric constant [37].

In what follows we use the Wannier states in Eq. (6) to derive the electric susceptibility and hence the linear absorbance, thereby recasting the Elliott formula for gapped Dirac materials. To solve Eq. (4) we expand the microscopic polarization in terms of these Wannier states; after a lengthy but straightforward calculation [20] we obtain

$$\vec{P}(\mathbf{r},\omega) = -\mathcal{E}(\omega)L^2\sum_\nu \frac{\int\vec{\Psi}^\dagger_\nu(\mathbf{r})\cdot\vec{\mu}_{cv}(\mathbf{r})d\mathbf{r}}{\hbar\omega - \hbar\omega_\nu + i\delta}\vec{\Psi}_\nu(\mathbf{r}). \tag{8}$$

Here $\vec{\mu}_{cv}(\mathbf{r}) = \mu_{cv}(\mathbf{r})\binom{1}{1}$ is the electric dipole in spinor form, $\mathcal{E}(\omega)$ is the electric field in the frequency domain, L^2 is the area of the sample, and δ is an energy broadening. We can now define the macroscopic polarization as follows:

$$P(\omega) = \int\left[\vec{\mu}^\dagger_{cv}(\mathbf{r})\cdot\vec{P}(\mathbf{r},\omega) + \vec{P}^{\,\dagger}(\mathbf{r},-\omega)\cdot\vec{\mu}_{cv}(\mathbf{r})\right]d\mathbf{r}, \tag{9}$$

and inserting Eq. (8), we get

$$P(\omega) = -L^2\,\mathcal{E}(\omega)\sum_\nu\frac{|\mathcal{I}_\nu|^2}{\hbar\omega - \hbar\omega_\nu + i\delta}, \tag{10}$$

where the oscillator strength is given by

$$|\mathcal{I}_\nu|^2 = \left|\int\mu_{cv}(\mathbf{r})[e^{i(j+1/2)\phi_{\mathbf{r}}}F_\nu(r) + e^{i(j-1/2)\phi_{\mathbf{r}}}G_\nu(r)]d\mathbf{r}\right|^2. \tag{11}$$

From the definition of polarization in cgs units $P(\omega) = L^2 d\,\chi(\omega)\mathcal{E}(\omega)$, we finally obtain the electron-hole pair susceptibility as

$$\chi(\omega) = -\frac{1}{d}\sum_\nu\frac{|\mathcal{I}_\nu|^2}{\hbar\omega - \hbar\omega_\nu + i\delta}. \tag{12}$$

The nominal layer thickness d has to be introduced to compute the volume within which the dipoles are induced, but as we shall see, it falls out in the calculation of the absorbance $\mathcal{A}$, which is the absorption coefficient multiplied by the layer thickness d. The influence of this effective layer thickness on the excitonic ground state was studied in a recent work [38].

From Eq. (12), using the Sokhotski-Plemelj theorem, we obtain the final expression of the linear absorbance: the *relativistic Elliott formula* for Dirac materials,

$$\begin{aligned}\mathcal{A}(\Omega) = \pi\alpha\Omega\Bigg[&\sum_\nu|\mathcal{I}_\nu|^2\delta\left(\Omega - \frac{1}{\sqrt{1 + \frac{\alpha_c^2}{(n+\gamma)^2}}}\right)\\ &+ C(\Omega)\,\Theta(\Omega - 1)\Bigg],\end{aligned} \tag{13}$$

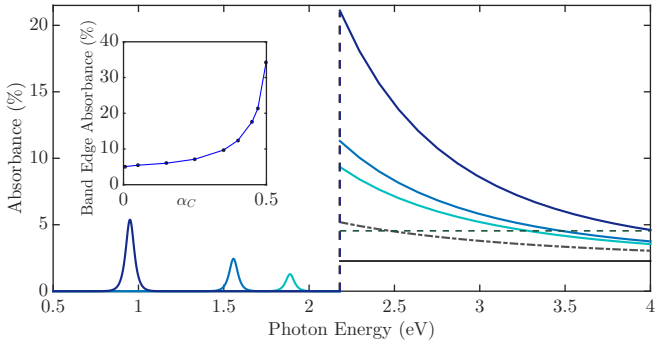

FIG. 2. Plot of the Elliott formula reducing the strength of the Coulomb coupling constant α_c. Dark blue, $\alpha_c = 0.45$; blue, $\alpha_c = 0.30$; cyan, $\alpha_c = 0.20$). Free-carrier limit, dash-dotted gray line; zero-gap graphene limit, solid black line; nonrelativistic free-carrier limit, dashed green line. Inset: Continuum absorbance at the band edge ($\Delta = 2.18$ eV) when increasing the strength of the Coulomb interactions.

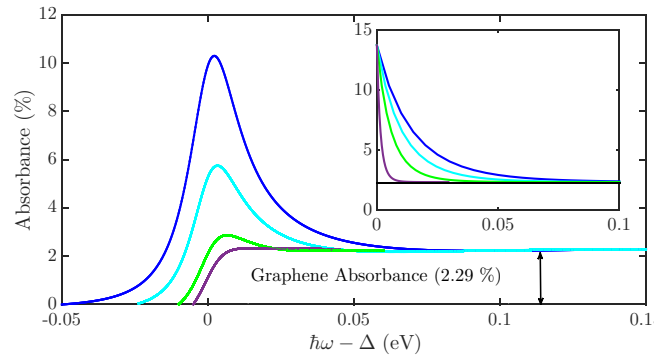

FIG. 3. Plot of the continuum absorbance contribution while reducing the band gap Δ ($\alpha_c = 0.35$) with a finite Lorentzian energy broadening $\delta = 10$ meV. Blue, $\Delta = 100$ meV; cyan, $\Delta = 50$ meV; green, $\Delta = 25$ meV; violet, $\Delta = 5$ meV. Inset: Continuum absorbance while reducing the band gap for zero-energy broadening ($\alpha_c = 0.35$). The axis labels are the same as in the main plot.

where $\Omega = \hbar\omega/\Delta$ is the scaled photon energy and Θ is the Heaviside step function. A similar formula was derived recently in Ref. [29], within a different formalism, in the same low-intensity and low-density limit but without considering the continuum states. We remark here the difference in the calculation of the dipole moment matrix element. We derived it directly from the Instantaneous eigenstates of the interacting Dirac equation, which allows us to account for the Berry phase and the dynamical symmetry breaking of the bands [21,32]. The two terms in Eq. (13) are the discrete and continuum contributions of the absorbance spectrum. Despite its striking similarity to the nonrelativistic case Eq. (13) is not trivial to evaluate since the integral given in Eq. (11) cannot be solved in closed form and must be evaluated numerically with particular care (some details about the structure of the dipole moment are given in Appendix C). The factor $C(\Omega)$ in the second term in Eq. (13) is what we may call the *relativistic Sommerfeld factor*:

$$C(\Omega) = \sum_{\nu} \frac{\Omega}{\sqrt{\Omega^2 - 1}} |\mathcal{I}_{\nu}(\Omega)|^2, \tag{14}$$

where the sum extends over the continuum states. This quantifies how the presence of electron-hole interactions enhances the continuum absorbance with respect to the free-carrier limit [20]. It is maximum at the energy gap ($\Omega = 1$) with a value that depends on the coupling constant α_c and tends to unity as the photon energy increases. This behavior is closely related to the relativistic energy spectrum and to the structure of the electron-hole continuum wave function, in contrast to the nonrelativistic case, which has a value of 2 at the band edge.

We now use Eq. (13) to demonstrate the development of the Coulomb effects on the absorbance spectrum for varying dielectric screenings and energy gaps. In Fig. 2 we plot the absorbance spectrum while varying the strength of the Coulomb interaction α_c. Experimentally, it is possible to tune the strength of the Coulomb interaction by changing the substrate on which the sample is deposited since it changes the overall dielectric constant. As expected, the binding energy and oscillator strength of the bound-state exciton lines decrease as the Coulomb interaction weakens (i.e., reducing α_c). For the continuum states, the Coulomb enhancement (Sommerfeld factor) is strongest at the band edge [see Eq. (14)]. Approaching the zero Coulomb limit ($\alpha_c = 0$), Eq. (13) reproduces exactly the free-carrier absorbance spectrum that can be computed analytically as $\mathcal{A}(\Omega) = \pi\alpha\,(\Omega^2 + 1)/\Omega^2$. As can be seen from the dash-dotted line in Fig. 2, this noninteracting model is unable to reproduce the giant continuum absorbance seen in experiment. It is therefore clear that the giant absorption of Dirac media such as TMDs is due to Coulomb interactions. The absorbance decreases quite rapidly as the photon energy is increased, and at high photon energy the absorbance approaches the universal (graphene) absorbance value of 2.3%. In this limit the high-energy electron and hole scattering wave functions involved are essentially identical to the free-particle wave functions. The inset in Fig. 2 shows how the absorbance at the band gap varies with α_c. We can clearly observe that it increases dramatically as the coupling constant approaches the critical value ($\alpha_c = 0.5$) where a phase transition to an excitonic insulator occurs [12,13,39]. This phase transition is a fundamental signature of purely Dirac excitons, and it potentially represents a measure of the *Diracness* [40] of the two-body electron-hole system since it disappears for a parabolic exciton dispersion [14].

One of the most remarkable features of graphene from a physics point of view is that there appears to be no Coulomb enhancement of the continuum absorbance, despite the existence of final-state Coulomb interactions. Figure 3 shows the continuum absorbance calculated from Eq. (13) while varying the energy gap Δ. We observe that on reducing the band gap, the curves approach the universal absorbance value of graphene $\pi\alpha$ at lower and lower photon energies. This indicates that the relevance of Coulomb interactions is confined to a region close to the energy gap, and once the gap is closed, the system behaves as a nearly-free-electron gas, as seen in experiments [4] and in the paper by Das Sarma and colleagues [41] by using a renormalization group approach. Within our theoretical approach this phenomenon can be explained by observing that in the relativistic hydrogenic model the energy

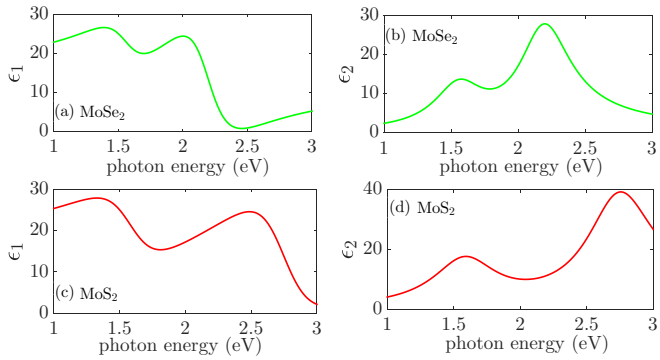

FIG. 4. (a) Real part of the dielectric function of $MoSe_2$. (b) Imaginary part of the dielectric function of $MoSe_2$. (c) Real part of the dielectric function of MoS_2. (d) Imaginary part of the dielectric function of MoS_2. This figure shows good agreement with the results in Figs. 1(e), 1(i), 1(g), and 1(k) of [19].

gap is the exact analog of the Rydberg constant that is the only relevant energy scale. This means that tuning the gap changes the relevant energy scale of the system; when it is reduced to zero, all photon-mediated transitions can be considered high-energy transitions, and in this regime the system is known to reproduce the free absorbance limit.

We shall now compare the results of our theoretical predictions with previous experimental results. To do so we compute the real and imaginary parts of the dielectric function for $MoSe_2$ and MoS_2 on a fused-silica substrate, and we compare our calculations with the experimental results in [19] (Fig. 4). The complex dielectric function is simply given by

$$\epsilon(\omega) = \epsilon_b + 4\pi\chi(\omega), \tag{15}$$

where ϵ_b is the background dielectric constant of the substrate. Here, we assume a thickness $d = 1$ nm for the monolayers since current experimental practice is to consider a two-dimensional crystal equivalent to a homogeneous slab with a nominal effective thickness. A more rigorous approach would be to consider the actual surface susceptibility, directly derived from Eq. (B17), and compare it with the data extracted from ellipsometric measurements [42].

IV. CONCLUSIONS

In conclusion we studied the linear optical properties of two-dimensional gapped Dirac materials. We derived a system of Coulomb-renormalized Dirac Bloch equations based on the quantization of instantaneous eigenstates. We provided an explicit expression of the absorbance Elliott formula for both the bound and continuum states within the generalized formalism of the quantized instantaneous eigenstates. We demonstrated how the absorbance spectrum evolves as the energy gap and the strength of Coulomb interaction are reduced to zero. In particular we showed that even in the presence of relatively strong electron-hole Coulomb interactions the gap reduction leads to universal absorbance, and we related this to the structure of the relativistic hydrogenic problem. Our theoretical framework will potentially be used to predict the behavior of the interaction of ultrashort pulses with Dirac media in a variety of experimental situations, leading to a fresh understanding of mechanisms of higher-harmonic generation and the study of cavities, multilayers, and TMD-enhanced microresonators.

ACKNOWLEDGMENTS

We would like to thank Prof. B. Gerardot (HWU) and his group for useful discussions. L.D.M.V. acknowledges support from EPSRC (UK, Grant No. EP/L015110/1) under the auspices of the Scottish Centre for Doctoral Training in Condensed Matter Physics.

APPENDIX A: QUANTIZATION OF THE INSTANTANEOUS DIRAC FIELD AND RENORMALIZED DIRAC-BLOCH EQUATIONS

The starting point of our analysis is the low-energy Hamiltonian for the band structure in the vicinity of the Dirac points. Dictated by the symmetry properties of the hexagonal lattice, the lowest- order $\mathbf{k}\cdot\mathbf{p}$ Hamiltonian including the light-matter interaction has the form

$$H^{\xi}_{\mathbf{k}} = H^{\xi}_{\mathbf{k},D} + H_C = v_F\left[\boldsymbol{\sigma}_{\xi}\cdot\left(\hat{\mathbf{p}}+\frac{e}{c}\mathbf{A}(t)\right)\right]+\sigma_z\frac{\Delta}{2}+\hat{I}_2 V(\mathbf{r}), \tag{A1}$$

where ξ is a valley index referring to the Dirac points ($\mathbf{K}$, $\mathbf{K}'$), $\boldsymbol{\sigma} = (\xi\sigma_x, \sigma_y)$ are the first two Pauli matrices, and σ_z is the third one. Since we are not considering the effect of the spin-orbit coupling, we can restrict ourselves to a single valley, namely, $\xi = 1$. Here, with letters D and C we indicate the interacting Dirac Hamiltonian and the Coulomb Hamiltonian, respectively. The aim of this appendix is to derive a renormalized system of Dirac-Bloch (RDB) equations from the second quantized form of the Hamiltonian in Eq. (A1). In order to do so we consider the following interacting Dirac equation:

$$i\hbar\frac{\partial}{\partial t}\vec{\psi}(\mathbf{r},t) = \left\{v_F\left[\boldsymbol{\sigma}\cdot\left(i\hbar\nabla+\frac{e}{c}\mathbf{A}(t)\right)\right]+\sigma_z\frac{\Delta}{2}\right\}\vec{\psi}(\mathbf{r},t). \tag{A2}$$

An ansatz solution to this equation can be given in terms of instantaneous eigenstates of the secular equation

$$H_{\mathbf{k},D}\vec{u}_{\lambda,\mathbf{k}}(t) = \epsilon_{\lambda,\mathbf{k}}\vec{u}_{\lambda,\mathbf{k}}(t). \tag{A3}$$

These eigenstates can be written in the normalized form

$$\vec{u}_{\lambda,\mathbf{k}}(t) = \frac{v_F|\boldsymbol{\pi}_k|}{\sqrt{\epsilon_{\mathbf{k}}(\lambda\Delta+2\epsilon_{\mathbf{k}})}}\begin{pmatrix}\frac{\lambda\Delta+2\epsilon_{\mathbf{k}}}{2v_F|\pi_{\mathbf{k}}|}e^{-i\phi_{\mathbf{k}}/2}\\ e^{i\phi_{\mathbf{k}}/2}\end{pmatrix}, \tag{A4}$$

where $|\boldsymbol{\pi}_{\mathbf{k}}| = \mathbf{p}+\frac{e}{c}\mathbf{A}(t)$, $\phi_{\mathbf{k}} = \arctan(\pi_x/\pi_y)$, and $\lambda = \pm 1$ label the conduction and valence bands. $\epsilon_{\mathbf{k}}(t)$ is the positive branch of the instantaneous energy:

$$\epsilon_{\lambda,\mathbf{k}} = \lambda\sqrt{\left(\frac{\Delta}{2}\right)^2+(v_F|\boldsymbol{\pi}_{\mathbf{k}}|)^2}. \tag{A5}$$

The introduction of the gap leads to an inequivalence of $\mathbf{K}$ and $\mathbf{K}'$ sublattices and, consequently, to the appearance of a Berry phase $\gamma_{\lambda,\mathbf{k}}(t) = \int_{-\infty}^{t} d\tau\, \vec{u}^{\dagger}_{\lambda,\mathbf{k}}(\tau)\cdot\dot{\vec{u}}_{\lambda,\mathbf{k}}(\tau)$. Consequently, the spinor (A4) evolves in time as follows:

$$\vec{\psi}_{\lambda,\mathbf{k}}(\mathbf{r},t) = \vec{u}_{\lambda,\mathbf{k}}(t)e^{-\lambda i[\theta_{\mathbf{k}}(t)-\gamma_{\mathbf{k}}(t)]+i\mathbf{k}\cdot\mathbf{r}}, \tag{A6}$$

where $\theta_{\mathbf{k}}(t) = \frac{1}{\hbar}\int_{-\infty}^{t} \epsilon_{\mathbf{k}}(\tau)d\tau$ is the *dynamical* phase and $\gamma_{\mathbf{k}}(t)$ is the positive-branch Berry phase. The Dirac field $\vec{\psi}(\mathbf{r}, t)$ can then be expanded in terms of instantaneous eigenstates,

$$\vec{\psi}(\mathbf{r}, t) = \sum_{\mathbf{k},\lambda=\pm 1} a_{\mathbf{k},\lambda}\vec{u}_{\mathbf{k},\lambda}e^{-\lambda i[\theta_{\mathbf{k}}(t)-\gamma_{\mathbf{k}}(t)]+i\mathbf{k}\cdot\mathbf{r}}, \tag{A7}$$

where $a_{\mathbf{k},\lambda}$ are band electron ladder operators. Substituting this field in the Hamiltonian

$$H_D = \int d\mathbf{r}\,\vec{\psi}^{\dagger}(\mathbf{r}, t)\left\{v_F\left[\boldsymbol{\sigma}\cdot\left(\nabla + \frac{e}{c}\mathbf{A}(t)\right)\right] + \sigma_z\frac{\Delta}{2}\right\}\vec{\psi}(\mathbf{r}, t) \tag{A8}$$

and introducing the hole operators $b^{\dagger}_{-\mathbf{k}} = a_{\mathbf{k},-1}$, after a lengthy but simple algebraic calculation we get the final form of the second quantized Hamiltonian:

$$H_D = \sum_{\mathbf{k}}[\epsilon_{\mathbf{k}}(t)\omega_k(t)(\hat{a}^{\dagger}_{\mathbf{k}}\hat{a}_{\mathbf{k}} - \hat{b}_{-\mathbf{k}}\hat{b}^{\dagger}_{-\mathbf{k}}) - \hbar\Omega_{\mathbf{k}}(t)(\hat{a}^{\dagger}_{\mathbf{k}}\hat{b}_{-\mathbf{k}} + \hat{b}^{\dagger}_{-\mathbf{k}}\hat{a}_{\mathbf{k}})], \tag{A9}$$

where $\Omega_{\mathbf{k}}(t)$ is a generalized Rabi frequency given by

$$\Omega_{\mathbf{k}}(t) = -i\vec{u}^{\dagger}_{\mathbf{k},1}\cdot\vec{u}_{\mathbf{k},-1} = \frac{ev_F E(t)}{\hbar}\left[\frac{\sin\phi_{\mathbf{k}}}{2\epsilon_{\mathbf{k}}} - i\Delta\frac{\cos\phi_{\mathbf{k}}}{4\epsilon^2_{\mathbf{k}}}\right]. \tag{A10}$$

Introducing the Coulomb interactions in the Hamiltonian, we get

$$\begin{aligned} H = &\sum_{\mathbf{k}}[\epsilon_k(t)(\hat{a}^{\dagger}_{\mathbf{k}}\hat{a}_{\mathbf{k}} - \hat{b}^{\dagger}_{-\mathbf{k}}\hat{b}_{-\mathbf{k}}) - \hbar\Omega_{\mathbf{k}}(t)(\hat{a}^{\dagger}_{\mathbf{k}}\hat{b}_{-\mathbf{k}} + \hat{b}^{\dagger}_{-\mathbf{k}}\hat{a}_{\mathbf{k}})] \\ &+ \frac{1}{2}\sum_{\mathbf{k},\mathbf{k}'}\sum_{\mathbf{p}\neq 0} V_{\mathbf{p}}(\hat{a}^{\dagger}_{\mathbf{k}+\mathbf{p}}\hat{a}^{\dagger}_{\mathbf{k}'-\mathbf{p}}\hat{a}_{\mathbf{k}'}\hat{a}_{\mathbf{k}} + \hat{b}^{\dagger}_{\mathbf{k}'+\mathbf{p}}\hat{b}^{\dagger}_{\mathbf{k}'-\mathbf{p}}\hat{b}_{-\mathbf{k}'}\hat{b}_{-\mathbf{k}} \\ &- 2\hat{a}^{\dagger}_{\mathbf{k}+\mathbf{p}}\hat{b}^{\dagger}_{\mathbf{k}'-\mathbf{p}}\hat{b}_{-\mathbf{k}'}\hat{a}_{\mathbf{k}}), \end{aligned} \tag{A11}$$

where $V_{\mathbf{p}}$ is the Coulomb potential in momentum space; we can now derive the equations for the population and inversion variables $n^e_{\mathbf{k}} = \langle\hat{a}^{\dagger}_{\mathbf{k}}\hat{a}_{\mathbf{k}}\rangle$, $n^h_{\mathbf{k}} = \langle\hat{b}^{\dagger}_{-\mathbf{k}}\hat{b}_{-\mathbf{k}}\rangle$, and $p_{\mathbf{k}} = \langle b_{-\mathbf{k}}a_{\mathbf{k}}\rangle$. This lengthy procedure is quite standard and can be found in any book on semiconductor theory (for example, [20]). It results in the following set of RDB equations:

$$\begin{aligned} \hbar\dot{p}_{\mathbf{k}} &= -2i\epsilon^R_{\mathbf{k}}(t)p_{\mathbf{k}} - i\hbar\Omega^R_{\mathbf{k}}(t)e^{i2\gamma_{\mathbf{k}}}\left(n^e_{\mathbf{k}} + n^h_{\mathbf{k}} - 1\right), \\ \dot{n}^{e,h}_{\mathbf{k}} &= -2\mathrm{Re}\left[\Omega^R_{\mathbf{k}}(t)\right]\mathrm{Im}(p_{\mathbf{k}}e^{i2\gamma_{\mathbf{k}}}) - 4\mathrm{Im}\left[\Omega^R_{\mathbf{k}}(t)\right]\mathrm{Re}(p_{\mathbf{k}}e^{i2\gamma_{\mathbf{k}}}), \end{aligned} \tag{A12}$$

where $\epsilon^R_{\mathbf{k}}(t) = \epsilon_{\mathbf{k}}(t) + \sum_{\mathbf{k}'\neq\mathbf{k}} V_{|\mathbf{k}-\mathbf{k}'|}(n^e_{\mathbf{k}'} + n^h_{\mathbf{k}'} - 1)$ and $\Omega^R_{\mathbf{k}}(t) = \Omega_{\mathbf{k}}(t) + 1/\hbar\sum_{\mathbf{k}'\neq\mathbf{k}} V_{|\mathbf{k}-\mathbf{k}'|}p_{\mathbf{k}'}$ are the renormalized energy and Rabi frequency.

APPENDIX B: THE WANNIER-DIRAC EQUATION

As in the case of 2D semiconductors, the Wannier equation can be derived from the RDB equations (A12). We consider the system under the approximation $e/cA(t) \ll \epsilon_g/(2v_F)$ and under the low-excitation approximation $w_k \approx -1$. Thus Eq. (A12) simplifies to

$$i\hbar\dot{p}_{\mathbf{k}} = -\left(2\epsilon_{\mathbf{k}} + \sum_{\mathbf{k}'\neq\mathbf{k}} V_{|\mathbf{k}-\mathbf{k}'|}\right)p_{\mathbf{k}} + \hbar\Omega_{\mathbf{k}}(t)e^{2i\gamma_{\mathbf{k}}}, \tag{B1}$$

with the nonrenormalized energy reducing to $\sqrt{v_F^2\mathbf{p}^2 + \Delta^2/4}$. This equation represents a two-dimensional, relativistic, two-particle system with an inhomogeneous term given by the optical field. In order to define the differential operator in the square root we write Eq. (B1) as follows:

$$\begin{aligned} i\hbar\frac{\partial}{\partial t}q_a(\mathbf{k}, t) = &\left[\hbar v_F(\alpha_i)_{ab}k_i + \beta_{ab}Mv_F^2\right]q_b(\mathbf{k}, t) \\ &+ i\sum_{\mathbf{k}'\neq\mathbf{k}} V_{|\mathbf{k}'-\mathbf{k}|}q_a(\mathbf{k}', t) - E(t)\mu_{\mathbf{k}}\gamma_a, \end{aligned} \tag{B2}$$

where $\hat{\alpha}_i$ and $\hat{\beta}$ are matrices with $a, b = (1, 2)$, $\vec{\gamma}$ is a spinor, and the mass parameter is $M = \Delta/(2v_F^2)$. Here, with $q_a(\mathbf{k}, t)$ we indicate the components of a spinor that represents the Wannier exciton eigenfunction in momentum space. Mathematically, this is fully analog to the definition of the Dirac spinor equation starting from the Schrödinger equation for a relativistic dispersion [43].

The dispersion in Eq. (B2) must satisfy

$$\hbar v_F(\alpha_i)_{ab}k_i + \beta_{ab}Mv_F^2 = \epsilon_{\mathbf{k}}\delta_{ab}. \tag{B3}$$

Thus we must have

$$\{\hat{\alpha}_i, \hat{\alpha}_j\} = \delta_{ij}, \quad (\hat{\alpha}_i)^2 = (\hat{\beta})^2 = \hat{I}_2. \tag{B4}$$

This algebra is satisfied by taking $(\tilde{\alpha}_1, \tilde{\alpha}_2) = (\sigma_x, \sigma_y)$ and $\tilde{\beta} = \sigma_z$. To determine the spinor $\vec{\gamma}$ we can switch off the Coulomb potential and impose that each component q_μ satisfy a Klein-Gordon equation with an inhomogeneous term $\mu_k E(t)$. To accomplish this it is sufficient to take $\vec{\gamma} = \binom{1}{1}$.

Taking the Fourier transform of Eq. (B2), we get

$$\begin{aligned} i\hbar\frac{\partial}{\partial t}\vec{q}(\mathbf{r}, t) = &\left[-iv_F\hbar\boldsymbol{\sigma}\cdot\nabla + \sigma_z Mv_F^2 + V(r)\right]\vec{q}(\mathbf{r}, t) \\ &+ E(t)\vec{\gamma}\mu(\mathbf{r}). \end{aligned} \tag{B5}$$

We shall now solve the homogeneous stationary eigenvalue problem

$$\left[-iv_F\hbar\boldsymbol{\sigma}\cdot\nabla + \sigma_z Mv_F^2 + V(r)\right]\vec{\Psi}_\nu(\mathbf{r}) = E_\nu\vec{\Psi}_\nu(\mathbf{r}), \tag{B6}$$

where ν indicates a set of quantum numbers. The solution to this equation is known (see, for example, [37]), and we report it here for completeness. It is convenient to solve the problem in polar coordinates. Writing the spinor in the form

$$\vec{\Psi}_\nu(\mathbf{r}) = \begin{pmatrix}\varphi_\nu \\ \chi_\nu\end{pmatrix}, \tag{B7}$$

we can write Eq. (B6) in spinor components (we will drop, for the moment, the quantum number subscript),

$$\begin{aligned} [E_c - k_c - U(r)]\phi &= (\partial_x - i\partial_y)\chi, \\ [E_c + k_c - U(r)]\chi &= (\partial_x + i\partial_y)\phi, \end{aligned} \tag{B8}$$

where we introduced the Compton units $E_c = E_n/(\hbar v_F)$ and $k_c = Mv_F/\hbar$ and $U = V/(\hbar v_F) = -e/(\hbar v_F r) = -\alpha_c/r$. The coupling constant α_c is then recomputed accounting for

the background dielectric constant ϵ_b that rescales the electric charge as $e \to e^* = e/(\epsilon_b - 1)$.

In polar coordinates we have $\partial_x \pm i\partial_y = e^{i\phi_{\mathbf{r}}}(\partial_r \pm 1/rL_z)$. where L_z is the third component of the angular momentum operator $\mathbf{L} = (0, 0, L_z)$. We can now write the spinor in Eq. (B7) in the form

$$\vec{\Psi}(\mathbf{r}) = \begin{pmatrix} e^{i(j+1/2)\phi_{\mathbf{r}}} F(r) \\ \pm i e^{i(j-1/2)\phi_{\mathbf{r}}} G(r) \end{pmatrix}, \tag{B9}$$

where $j = m + 1/2$ is the eigenvalue of the isospin-angular momentum $\hat{J}_z = \hat{L}_z + \frac{1}{2}\sigma_z$ along the z axis. Substituting the spinor (B9) in Eq. (B6), we get the radial equations

$$\begin{aligned} &\frac{d}{dr}F - \frac{j}{r}F + (E_c + k_c - U)G = 0, \\ &\frac{d}{dr}G - \frac{j}{r}G + (E_c - k_c - U)F = 0. \end{aligned} \tag{B10}$$

In spite of its apparent simplicity the solution of this system is far from being trivial. One way to solve it is to decouple it into two independent second-order differential equations; to do so we write the solution in the following form:

$$\begin{aligned} F(r) &= (k_c + E_c)^{1/2} e^{-\lambda r} (2\lambda r)^{\gamma - 1/2} \tilde{F}(r), \\ G(r) &= (k_c - E_c)^{-1/2} e^{-\lambda r} (2\lambda r)^{\gamma + 1/2} \tilde{G}(r), \end{aligned} \tag{B11}$$

with $\kappa = \sqrt{k_c^2 - E_c^2}$ and $\gamma = \sqrt{j^2 - \alpha_c^2}$. Introducing the dimensionless radius $\rho = 2\lambda r$, we get

$$\begin{aligned} &\rho\frac{d}{d\rho}\tilde{F} + (\gamma - j)\tilde{F} - \frac{\rho}{2}(\tilde{F} - \tilde{G}) + \frac{\kappa\alpha_c}{k_c + E_c}\tilde{G} = 0, \\ &\rho\frac{d}{d\rho}\tilde{G} + (\gamma + j)\tilde{G} - \frac{\rho}{2}(\tilde{F} - \tilde{G}) + \frac{\kappa\alpha_c}{k_c - E_c}\tilde{G} = 0. \end{aligned} \tag{B12}$$

Writing $\tilde{F} = Q_1 + Q_2$ and $\tilde{G} = Q_1 - Q_2$, we find

$$\begin{aligned} &\rho\frac{d}{d\rho}Q_1 + \left(\gamma - \frac{\alpha_c E_c}{\kappa}\right)Q_1 - \left(j + \frac{k_c\alpha_c}{\kappa}\right)Q_2 = 0, \\ &\rho\frac{d}{d\rho}Q_2 + \left(\gamma - \rho + \frac{\alpha_c E_c}{\kappa}\right)Q_2 - \left(j - \frac{k_c\alpha_c}{\kappa}\right)Q_1 = 0; \end{aligned} \tag{B13}$$

looking at this system at $\rho = 0$, we derive the useful relation

$$\gamma^2 - \left(\frac{\alpha_c E_c}{\kappa}\right)^2 = j^2 - \left(\frac{k_c\alpha_c}{\kappa}\right)^2. \tag{B14}$$

Using (B14), we can easily decouple the system, obtaining

$$\begin{aligned} &\rho\frac{d^2}{d\rho^2}Q_1 + (1 + 2\gamma - \rho)\frac{d}{d\rho}Q_1 - \left(\gamma - \frac{\alpha_c E_c}{\kappa}\right)Q_1 = 0, \\ &\rho\frac{d^2}{d\rho^2}Q_2 + (1 + 2\gamma - \rho)\frac{d}{d\rho}Q_2 - \left(1 + \gamma - \frac{\alpha_c E_c}{\kappa}\right)Q_2 = 0. \end{aligned} \tag{B15}$$

These equations are in the confluent hypergeometric form

$$z^2\frac{d^2}{dz^2}f + (b - z)\frac{d}{dz}f - af = 0. \tag{B16}$$

One solution is given in terms of the Kummer hypergeometric function ${}_1\mathcal{F}_1(a, b; z)$ [44]. Thus Q_1 and Q_2 are given by

$$\begin{aligned} Q_1 &= C^{(1)}{}_1\mathcal{F}_1(\gamma - \alpha_c E_c/\kappa, 1 + 2\gamma; \rho), \\ Q_2 &= C^{(2)}{}_1\mathcal{F}_1(1 + \gamma - \alpha_c E_c/\kappa, 1 + 2\gamma; \rho). \end{aligned} \tag{B17}$$

Since ${}_1\mathcal{F}_1(a, b, 0) = 1$, looking again at (B13) for $\rho = 0$, we get

$$c^{(12)} = \frac{C^{(1)}}{C^{(2)}} = \frac{\gamma - \alpha_c E_c/\kappa}{j + k_c\alpha_c/\kappa}. \tag{B18}$$

Thus we can write the eigenfunctions for the discrete spectrum ($\nu = n, j$),

$$\begin{aligned} F_\nu &= (k_c + E_c)^{1/2} e^{-\rho/2} \rho^{\gamma - 1/2} C^{(1)} [{}_1\mathcal{F}_1(\gamma - \alpha_c E_c/\kappa, 1 + 2\gamma; \rho) + c^{(12)}{}_1\mathcal{F}_1(1 + \gamma - \alpha_c E_c/\kappa, 1 + 2\gamma; \rho)], \\ G_\nu &= (k_c - E_c)^{1/2} e^{-\rho/2} \rho^{\gamma - 1/2} C^{(1)} [{}_1\mathcal{F}_1(\gamma - \alpha_c E_c/\kappa, 1 + 2\gamma; \rho) - c^{(12)}{}_1\mathcal{F}_1(1 + \gamma - \alpha_c E_c/\kappa, 1 + 2\gamma; \rho)]. \end{aligned} \tag{B19}$$

The bound states occur when the first argument of the hypergeometric function is a negative integer, i.e.,

$$\gamma - \frac{\alpha_c E_c^\nu}{\kappa} = -n; \tag{B20}$$

from this equation we directly obtain the discrete spectrum

$$E_c^\nu = \frac{k_c}{\sqrt{1 + \frac{\alpha_c^2}{(n+\gamma)^2}}}. \tag{B21}$$

Using *Mathematica*, we can find the normalization factor from the condition

$$\int d\mathbf{r}\, \vec{\Psi}^\dagger(\mathbf{r})\vec{\Psi}(\mathbf{r}) = 2\pi \int_0^\infty r dr\, (F^2 + G^2) = 1, \tag{B22}$$

and we get

$$C^{(1)} = \frac{(-1)^n \kappa^{3/2}}{2\pi k_c \Gamma(1 + 2\gamma)} \sqrt{\frac{\Gamma(1 + 2\gamma + n)(j + k_c\alpha_c/\lambda)}{\alpha_c n!}}. \tag{B23}$$

We now compute the continuum states of the system by analytic continuation of the eigenfunctions of the Wannier equation in the region $|E| > \Delta/2$, i.e., for complex values of κ. Switching back to Compton units, the analytic continuation in the E_c complex plane is easily accomplished by

$$\begin{aligned} &\kappa = \sqrt{k_c^2 - E_c^2} \to -ik, \quad k = \sqrt{E_c^2 - k_c^2}, \\ &c_{12} \to e^{-2i\xi_j} = \frac{\gamma - i\alpha_c^E}{j + iM\alpha_c/k}, \quad \alpha_c^E = \frac{\alpha_c E}{k}. \end{aligned} \tag{B24}$$

Substituting this prescription in the eigenfunctions and after lengthy but straightforward calculations [37], we get

$$F = 2\sqrt{\frac{|E_c + k_c|}{\pi E_c}}\frac{\left|\Gamma\left(1+\gamma+i\alpha_c^E\right)\right|}{\Gamma(1+2\gamma)}e^{\pi\alpha_c^E/2}(2kr)^{\gamma-1/2} \times \mathrm{Re}\left\{e^{ikr+i\xi}{}_1\mathcal{F}_1\left(\gamma - i\alpha_c^E, 1+2\gamma; -2ikr\right)\right\},$$

$$G = \pm 2\sqrt{\frac{|E_c - k_c|}{\pi E_c}}\frac{\left|\Gamma\left(1+\gamma+i\alpha_c^E\right)\right|}{\Gamma(1+2\gamma)}e^{\pi\alpha_c^E/2}(2kr)^{\gamma-1/2} \times \mathrm{Im}\left\{e^{ikr+i\xi}{}_1\mathcal{F}_1\left(\gamma - i\alpha_c^E, 1+2\gamma; -2ikr\right)\right\}. \quad \text{(B25)}$$

Both the discrete and continuum eigenstates derived here are used in the paper for the calculation of the Elliott formula.

APPENDIX C: THE OPTICAL MATRIX ELEMENT

It is useful to compute the dipole moment in the position space. Using the more manageable Compton units, we get

$$\mu(\mathbf{r}) = \frac{L^2}{(2\pi)^2}\int d\mathbf{k}\,\mu_{\mathbf{k}}e^{i\mathbf{k}\cdot\mathbf{r}} = e\frac{L^2}{2\pi^2}\int_0^\infty kdk \times \int_0^{2\pi} d\phi_{\mathbf{r}}e^{ikr(\phi_{\mathbf{k}}-\phi_{\mathbf{r}})}\left(\frac{\sin\phi_{\mathbf{k}}}{\sqrt{k^2+k_c^2}} - ik_c\frac{\cos\phi_{\mathbf{k}}}{k^2+k_c^2}\right). \quad \text{(C1)}$$

This integral converges and can be solved analytically. With *Mathematica* we get

$$\mu(\mathbf{r}) = e\frac{L^2}{(2\pi)^2}\left[k_c\pi^2\cos(\phi_{\mathbf{r}})[I_1(k_cr) - S_{-1}(k_cr)] - i\sqrt{\pi}k_c\sin(\phi_{\mathbf{r}})G\left(0, -\frac{1}{2}, \frac{1}{2}, \frac{1}{2}\middle|\frac{(k_cr)^2}{4}\right)\right], \quad \text{(C2)}$$

where $G(a_n, b_n|z)$ is the Mejer G function and $S_\alpha(z)$ is the Struve function of order α. In the case of zero gap ($k_c \to 0$) the integral simplifies considerably, giving

$$\mu(\mathbf{r}) = i\frac{L^2}{(2\pi)^2}\frac{\sin\phi_{\mathbf{r}}}{r}. \quad \text{(C3)}$$

The dipole moment in Eq. (C2) is essential to compute the oscillator strength $|\mathcal{I}_v|^2$ defined in integral (11) of the main text. This integral is not trivial to compute due to the special functions in the dipole moment. In particular even if both the real and imaginary parts of $\mu(\mathbf{r})$ converge [44], the numerical implementation is problematic, in particular in the region $r \gg 1$. A way to solve this problem is to find a fit for these functions, in the large-r region, involving just simple polynomials and exponentials. Using *Mathematica*, we find the following best fit:

$$\frac{\mu_R(r)}{eL^2} \to ae^{-bk_cr}, \quad a = -0.048592,\ b = -0.780094,$$
$$\frac{\mu_I(r)}{eL^2} \to ce^{-k_cr} + d\frac{e^{-k_cr}}{(k_cr)^2} + \frac{e}{(k_cr)^2}, \quad c = -0.021511,$$
$$d = -0.071833,\ e = 0.027752, \quad \text{(C4)}$$

where with $\mu_{R,I}(r)$ we indicate the radial components of the real and imaginary parts of the dipole moment (Fig. 5). To compute the oscillator strength we thus use the exact dipole moment between 0 and $k_cr_{\mathrm{cut}} = 2$ and the fit between $k_cr_{\mathrm{cut}} = 2$ and $k_cr_{\mathrm{cut}} = 30$. We verified that integrating up to $k_cr_{\mathrm{cut}} = 30$ was enough for the numeric integral to converge.

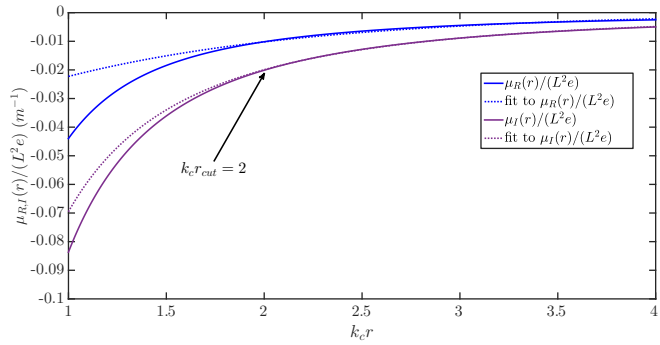

FIG. 5. Fit of the radial components of the real and imaginary parts of the dipole moment in units of area L^2 and electric charge e.

[1] T. O. Wehling, A. Black-Shaffer, and A. V. Balatsky, Adv. Phys. **63**, 1 (2013).
[2] K. S. Novoselov, A. K. Geim, S. V. Morozov, Y. Z. D. Jiang, S. V. Dubonos, I. V. Grigorieva, and A. A. Firsov, Science **306**, 666 (2004).
[3] K. S. Novoselov and A. K. Geim, Nature (London) **438**, 197 (2005).
[4] R. R. Nair, P. Blake, A. N. Grigorenko, K. S. Novoselov, T. J. Booth, T. Stauber, N. M. R. Peres, and A. K. Geim, Science **320**, 1308 (2008).
[5] T. Winzer, A. Knorr, and E. Malic, Nano Lett. **10**, 4839 (2010).
[6] S. Y. Zhou, G. Gweon, P. F. A. Fedorov, W. D. Heer, D.-H. Lee, F. Guinea, A. C. Neto, and A. Lanzara, Nat. Mater. **6**, 770 (2007).
[7] J. Kang, J. Bang, B. Ryu, and K. J. Chang, Phys. Rev. B **77**, 115453 (2008).
[8] Z. H. Ni, T. Yu, Y. H. Lu, Y. Y. Wang, Y. P. Feng, and Z. X. Shen, ACS Nano **2**, 2301 (2008).
[9] C. Cohen-Tannoudji, J. Dupont-Roc, and G. Grynberg, *Introduction to Quantum Electrodynamics* (Wiley, New York, 1989).
[10] M. I. Katsnelson, *Graphene: Carbon in Two Dimensions* (Cambridge University Press, Cambridge, 2012).
[11] D. Xiao, G. B. Liu, W. Feng, X. Xu, and W. Yao, Phys. Rev. Lett. **108**, 196802 (2012).
[12] A. S. Rodin and A. H. Castro Neto, Phys. Rev. B **88**, 195437 (2013).
[13] T. Stroucken and S. W. Koch, J. Phys.: Condens. Matter **27**, 345003 (2015).

[14] M. Trushin, M. O. Goerbig, and W. Belzig, Phys. Rev. B **94**, 041301 (2016).
[15] M. Trushin, M. O. Goerbig, and W. Belzig, Phys. Rev. Lett **120**, 187401 (2018).
[16] K. F. Mak, C. Lee, J. Hone, J. Shan, and T. F. Heinz, Phys. Rev. Lett. **105**, 136805 (2010).
[17] E. Cappelluti, R. Roldán, J. A. Silva-Guillén, P. Ordejón, and F. Guinea, Phys. Rev. B **88**, 075409 (2013).
[18] M. M. Ugeda, A. J. Bradley, S.-F. Shi, F. H. da Jornada, Y. Zhang, D. Y. Qiu, W. Rua, S.-K. Mo, Z. Hussain, Z.-X. Shen *et al.*, Nat. Mater. **13**, 1091 (2014).
[19] Y. Li, A. Chernikov, X. Zhang, A. Rigosi, H. M. Hill, A. M. van der Zande, D. A. Chenet, E.M. Shih, J. Hone, and T. F. Heinz, Phys. Rev. B **90**, 205422 (2014).
[20] H. Haug and S. W. Koch, *Quantum Theory of the Optical and Electronic Properties of Semiconductors* (World Scientific, Singapore, 1990).
[21] D. N. Carvalho, F. Biancalana, and A. Marini, Phys. Rev. B **97**, 195123 (2018).
[22] G. Berghäuser and E. Malic, Phys. Rev. B **89**, 125309 (2014).
[23] A. Steinhoff, M. Rösner, F. Jahnke, T. O. Wehling, and C. Gies, Nano Lett. **14**, 3743 (2014).
[24] M. L. Trolle, G. Seifert, and T. G. Pedersen, Phys. Rev. B **89**, 235410 (2014).
[25] D. Y. Qiu, F. H. da Jornada, and S. G. Louie, Phys. Rev. Lett. **111**, 216805 (2013).
[26] K. L. Ishikawa, Phys. Rev. B **82**, 201402 (2010).
[27] F. Xia, H. Wang, D. Xiao, M. Dubey, and A. Ramasubramaniam, Nat. Photonics **8**, 899 (2014).
[28] A. Ramasubramaniam, Phys. Rev. B **86**, 115409 (2012).
[29] A. J. Chaves, R. M. Ribeiro, T. Federico, and N. M. R. Peres, 2D Mater. **4**, 025086 (2017).
[30] E. Ridolfi, C. H. Lewenkopf, and V. M. Pereira, Phys. Rev. B **97**, 205409 (2018).
[31] M. Lindberg and S. W. Koch, Phys. Rev. B **38**, 3342 (1988).
[32] D. N. Carvalho, A. Marini, and F. Biancalana, Ann. Phys. (N.Y.) **378**, 24 (2017).
[33] M. Lindberg, R. Binder, and S. W. Koch, Phys. Rev. A **45**, 1865 (1992).
[34] J. Danckwerts, K. J. Ahn, J. Förstner, and A. Knorr, Phys. Rev. B **73**, 165318 (2006).
[35] B. Zaks, D. Stehr, T. A. Truong, P. M. Petroff, S. Hughes, and M. S. Sherwin, New J. Phys. **13**, 083009 (2011).
[36] G. B. Liu, W. Y. Shan, Y. Yao, W. Yao, and D. Xiao, Phys. Rev. B **88**, 085433 (2013).
[37] D. S. Novikov, Phys. Rev. B **76**, 245435 (2007).
[38] L. Meckbach, T. Stroucken, and S. W. Koch, Phys. Rev. B **97**, 035425 (2018).
[39] J. Grönqvist, T. Stroucken, M. Lindberg, and S. W. Koch, Eur. Phys. J. B **85**, 395 (2012).
[40] M. O. Goerbig, G. Montambaux, and F. Piécon, Eur. Phys. Lett. **105**, 57005 (2014).
[41] J. Hofmann, E. Barnes, and S. Das Sarma, Phys. Rev. Lett. **113**, 105502 (2014).
[42] G. Jarswal, Z. Dai, X. Zhang, M. Bagnarol, A. Martucci, and M. Merano, Opt. Lett. **43**, 703 (2018).
[43] L. Maiani and O. Benhar, *Relativistic Quantum Mechanics: An Introduction to Relativistic Quantum Fields* (CRC Press, Boca Raton, FL, 2015).
[44] F. Olver, *Asymptotics and Special Functions* (Academic Press, New York, 1974).